OsteoArthritis and Cartilage (2007) **15,** 169–178

doi:10.1016/j.joca.2006.06.021

Osteoarthritis and Cartilage

International Cartilage Repair Society

OARSI OSTEOARTHRITIS RESEARCH SOCIETY INTERNATIONAL

Comparison of mechanical debridement and radiofrequency energy for chondroplasty in an *in vivo* equine model of partial thickness cartilage injury[1]

R. B. Edwards III, D.V.M., Ph.D.†, Y. Lu M.D.‡*, R. K. Uthamanthil D.V.M., Ph.D.‡, J. J. Bogdanske B.A.‡, P. Muir B.V.Sc., Ph.D.†, K. A. Athanasiou Ph.D.§ and M. D. Markel D.V.M., Ph.D.‡

† *Comparative Orthopaedic Research Laboratory, Department of Surgical Sciences, School of Veterinary Medicine, University of Wisconsin-Madison, Madison, WI 53706-1102, USA*

‡ *Comparative Orthopaedic Research Laboratory, Department of Medical Sciences, School of Veterinary Medicine, University of Wisconsin-Madison, Madison, WI 53706-1102, USA*

§ *Musculoskeletal Bioengineering Laboratory, Department of Bioengineering, Rice University, Houston, TX 77005, USA*

Summary

Objective: The purpose of this study was to develop a long-term model of cartilage injury that could be used to compare the effects of radiofrequency energy (RFE) and mechanical debridement as a treatment.

Methods: Partial thickness fibrillation of patellar cartilage was created in 16 mature ponies. Three months after the initial surgery all injured patellae were randomly selected to receive one of the four treatments ($n = 8$/treatment): (1) control, (2) mechanical debridement with a motorized shaver, (3) TAC-CII RFE probe, and (4) CoVac 50 RFE probe. The ponies were euthanized 22 months after treatment. Macroscopic appearance of the cartilage surface was scored, vital cell staining was used to determine chondrocyte viability and light microscopy was used to grade the morphometric changes within the cartilage. Mechanical properties (aggregate modulus, Poisson's ratio and permeability) also were determined and compared to normal uninjured cartilage.

Results: There were no differences in the cartilage surface scores among the treatment groups and control samples ($P > 0.05$). The maximum depth of cell death and the percentage of dead area in control and mechanical debridement groups were significantly less than those in both RFE groups. There were no significant differences in maximum depth and the percentage of dead area between the two RFE treatment groups. Histologic scores demonstrated better cartilage morphology for the control and mechanical debridement groups than those of RFE groups. However, even with full thickness chondrocyte death, the matrix in the RFE treated sections was still retained and the mechanical properties of the treated cartilage did not differ from the mechanical debridement group.

Conclusion: RFE caused greater chondrocyte death and more severe morphological changes compared to untreated degenerative cartilage and mechanical debridement in this model.

Key words: Articular cartilage, Radiofrequency energy, Thermal chondroplasty, Confocal laser microscopy, Chondrocyte.

Introduction

Focal and diffuse partial thickness fibrillation, chondral fracture, and partial thickness erosion are commonly encountered by orthopedic surgeons and create significant pain and gradual loss of joint function for patients[1,2]. The intrinsic repair capabilities of cartilage are limited and the resulting tissue produced in adult patients is generally inferior to normal cartilage[3–5]. Historically, multiple treatment modalities have been used to address focal lesions and include arthroscopic lavage, laser thermal chondroplasty, subchondral microfracture, autogenous chondrocyte grafting, and mosaicplasty[6,7].

Appropriate animal models represent one of the obstacles to developing clinically successful cartilage repair therapies[8–10]. Numerous strategies have been developed for cartilage repair with varying degrees of success; however, complete, functional permanent repair has never been reported in the postnatal animal. Cartilage thickness varies considerably across species, anatomy varies due to quadruped vs biped mechanics, and healing may actually be faster in the human because of the ability to use postoperative rehabilitation techniques in combination with patient

[1]This study was funded by Smith & Nephew, Inc., Endoscopy Division, 150 Minuteman Road, Andover, MA 01810, USA; The National Football League, Medical Charities Grant, NFL, 280 Park Avenue, New York, NY 10017, USA; Houston Equine Research Organization, 7575 N. Sam Houston Parkway W., Houston, TX 77064-3417, USA.

*Address correspondence and reprint requests to: Dr Yan Lu, M.D., Comparative Orthopaedic Research Laboratory, Department of Medical Sciences, School of Veterinary Medicine, University of Wisconsin-Madison, 2015 Linden Drive, Madison, WI 53706-1102, USA. Tel: 1-608-265-7878; Fax: 1-608-265-8020; E-mail: luy@svm.vetmed.wisc.edu

Received 19 January 2006; revision accepted 30 June 2006.

compliance[10]. Furthermore, a principal outcome measure in the human, which is pain, can only be assessed indirectly in animals through measures such as heart rate, kinematic analysis or force plate analysis.

Radiofrequency energy (RFE) has been used for years in general surgery, neurosurgery, oncology, cardiology, ophthalmology, and most recently in musculoskeletal surgery for a variety of indications[11–13]. Currently 18% of articular cartilage debridement procedures involve the use of RFE. However, this remains a controversial treatment due to conflicting reports of clinical and *in vitro* and *in vivo* experimental studies[11,14–16]. The popularity of RFE has resulted from three major factors: the rapid smoothing and contouring of fibrillated cartilage without irregularities produced by motorized shavers, significant improvement in clinical signs after surgery with a low complication rate, and *in vivo* and *in vitro* reports demonstrating little to no chondrocyte injury or necrosis adjacent to the treated regions[14,17,18]. Further *in vivo* and *in vitro* work and clinical reviews have resulted in conflicting reports regarding the effects of RFE on articular cartilage and chondrocyte viability[19–24]. RFE can create a stable articular surface that has been demonstrated to resist surface fibrillation for up to 6 months after treatment overcoming the issues of excessive tissue removal and producing smoother, more rapid contouring than can be achieved with mechanical debridement[22]. These improvements over mechanical debridement have led to continued clinical use and set the challenge to develop better probes that allow surface contouring but avoid the undesirable effects such as cell death[25].

The purpose of this study was to utilize a large animal model that mimicked cartilage injury and the subsequent degenerative process, characterized by softening of the cartilage and partial thickness fibrillation of the cartilage surface. This model was then used to compare the treatments of mechanical debridement and RFE and determine the potential benefits of these treatments. Specifically, the macroscopic appearance of the cartilage surface, the long-term chondrocyte viability, and light microscopy were used to assess the effect of these treatments on injured cartilage compared to untreated control. In addition, there are no reports describing the long-term changes in mechanical properties of articular cartilage after RFE treatment. Recently, reports of *in vitro* application of low energy ($\leq$30 W) RFE on arthritic femoral articular cartilage showed no significant immediate differences in stiffness pre and posttreatment[26]. We hypothesized that the use of RFE for thermal chondroplasty would produce a stable articular surface with less surface fibrillation than mechanical shaving and enhanced long-term mechanical properties compared to mechanical debridement and untreated control, but would result in significant thermal injury to chondrocytes.

Materials and methods

Sixteen mature ponies, ranging in age from 4 to 6 years and weighing between 130 and 190 kg (147 ± 7; mean $\pm$ S.E.M) were used in this study. All experimental protocols were approved by the Institutional Animal Care and Use Committee. Following induction of general anesthesia, bilateral femoropatellar arthroscopy was performed as previously described[27,28]. A custom-designed, stainless steel abrading tool (4 mm $\times$ 4 mm with four cutting edges 500 μm in height) for roughening the cartilaginous surface of the patella was applied bilaterally to the patellar surface to create an abraded surface approximately 2×2 cm^2 that would approximate Grade 2–3 partial thickness cartilage injury with surface fibrillation and chondral fracture. After the initial surgery, the ponies were restricted to stall rest (20×20 feet stalls) for 14 days and then provided paddock turnout for 76 days. A second arthroscopic procedure using the previously described approach was performed 90 days after the cartilage abrasion and one of the four treatments (surgical control, TAC-CII RFE probe, CoVac 50 RFE probe and motorized shaving; $n = 8$ patellae/treatment group) was applied to each patellar surface as determined by presurgical random block design.

Untreated cartilage lesions in control joints were arthroscopically examined at 90 days after the cartilage abrasion, an instrument portal was established, and the fibrillated cartilage region on the patella was examined with a blunt probe. Prior to treatment, a 2.0-mm osteochondral biopsy was taken with a 13-gage Jamshidi biopsy instrument and placed in sterile PBS for analysis of cell viability and cartilage thickness by confocal laser microscopy. For the mechanical debridement group, the debridement was performed using a 3.5 mm oscillating blade (full radius resector, C9800, Linvatec Corporation, Largo, FL). The fronds in the fibrillated region were resected and an attempt was made to smooth the surface without removing excessive cartilage. RFE treatments were performed using a paintbrush pattern for both RFE devices. TAC-CII (Vulcan EAS coupled with TAC-CII probe at the setting of 70°C/15 W, Smith & Nephew, Endoscopy, Andover, MA) was applied in light contact, and the CoVac 50 (ArthroCare 2000 coupled with CoVac 50 probe at setting of 2, ArthroCare Corporation, Sunnyvale, CA) was used in short 2–3 s activation periods in a non-contact manner. The selected RFE settings were the manufacturers' recommended settings at the time of the study. Based on previously reported thermometry studies, continuous lavage (200-mL/min) was used during CoVac 50 application in an attempt to reduce surface heating. However, when the TAC-CII was used, lavage was stopped to prevent cooling of the RFE probe tip with concomitant increased power application[23]. For each 4 cm^2 degenerative area of the patella, the RFE treatment time was limited to contouring the surface and removing fine fibrillations. When large fronds were present, they were removed with grasping forceps before RFE was applied. Postoperative exercise restrictions were identical to the first surgery.

All ponies were euthanized 22 months after the second surgery. The patellae were harvested and photographed for evaluation of macroscopic appearance of the cartilaginous surfaces using a subjective scoring system by three senior researchers that were unaware of the treatments used (Table I). The patellae were cut by band saw irrigated with saline solution into smaller osteochondral blocks with

Table I
Macroscopic appearance of RFE treated cartilage surface

Macroscopic appearance of RFE treated cartilage surface	Score
No cartilage loss and smooth	4
No cartilage loss and relatively smooth	3
Minimal cartilage loss with rough and irregular surface	2
<25% Cartilage loss with minimal subchondral bone exposed	1
>25% Cartilage loss with substantial amount of exposed subchondral bone	0

at least 1.0 cm of subchondral bone for biomechanical, vital cell staining or histological analysis. A low-speed saw irrigated with saline solution (Buehler, Isomet 2000, Lake Bluff, IL) was used to cut the osteochondral block into slices with a thickness of 1.5 and 2.5 mm. The 1.5 mm thick slices were analyzed for chondrocyte viability by confocal laser microscopy on the day of the harvest. The 2.5 mm thick slices were used for histologic analysis by light microscopy.

BIOMECHANICAL ANALYSIS

Four osteochondral sections were collected for mechanical testing: the treated region, the upper border of treated region (border area), the same facet of the treated area (superiolateral area), and the opposite facet (medial area) of the patella (Fig. 1). All the sections were of at least 2.25 cm^2. The collected samples were wrapped in gauzes soaked in 0.9% NaCl solution with protease inhibitors (benzimidine hydrochloride, 5 mmol/L; *N*-methyl malamine 10 mmol/L; ethylene diamine tetra acetic acid 2 mmol/L; phenyl methyl sulphonyl flouride, 1 mmol/L) and stored at $-80^{\circ}C$.

Each specimen was thawed in 0.9% NaCl solution with protease inhibitors at room temperature for 1 h. Each osteochondral specimen was subjected to one freeze thaw cycle, which is not believed to affect the tissue's biomechanical properties[29]. The osteochondral specimens were tested with an automated creep indentation apparatus to obtain creep and recovery behavior of the articular cartilage[29–31]. For testing, each specimen was mounted with cyanoacrylate cement to the base of a bath, containing 0.9% NaCl with protease inhibitors. A flat ended, cylindrical, rigid, porous indenter tip of 1 mm diameter, made of sintered steel and having a much higher porosity than articular cartilage, was used. Perpendicularity of the indenter tip was achieved using a small cylindrical metallic bit with flat ends placed on the area to be tested on the surface of the sample. By carefully moving the stage, the indenter tip and the bit was positioned in co-linear alignment so that flat surfaces of both were made parallel to each other. Once surfaces of the indenter and the bit became parallel, the experiment was started after removing the bit. Perpendicularity was achieved in 30–60 s.

After equilibrium to a tare load of 0.0049 N was reached, a main load of 0.098 N was applied until equilibrium. The main load was then removed automatically at equilibrium and the recovery phase began under the tare load. After recovery equilibrium, the load was removed and the tissue was allowed to recover unloaded completely for 30 min in the solution. The thickness of the cartilage at the site of testing was measured using a needle probe[29–31]. Once the tissue resistance to the needle reached 2.45 N the needle was automatically withdrawn and the thickness was determined based on the graph plotted.

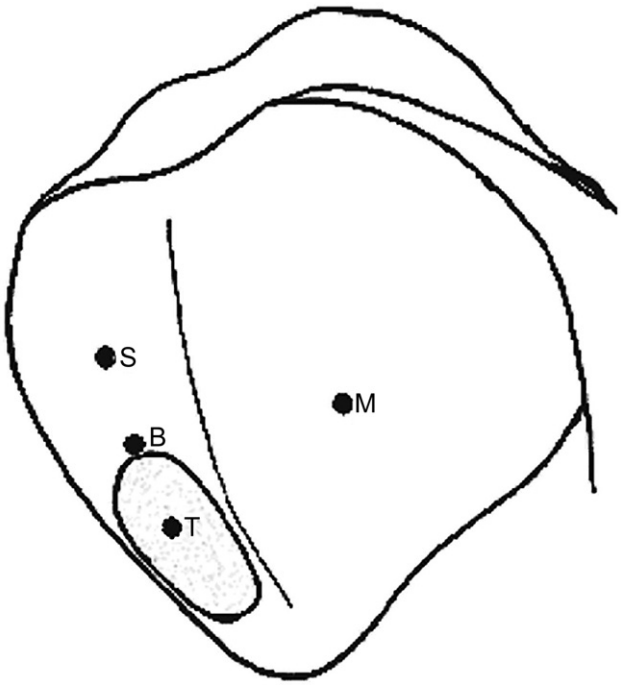

Fig. 1. Schematic of the articular surface of the patella demonstrating the treated region and the sites used for biomechanical testing: T – treated area, B – border between treated and untreated areas, S – superiolateral area, and M – medial area.

CONFOCAL LIGHT MICROSCOPY

Cell viability was determined using previously described techniques using 0.4 μl calcein (acetoxymethylester)/10 μl ethidium homodimer (Molecular Probes, Eugene, OR)[22,32,33]. A confocal laser microscope (MRC-1024, Bio-Rad, Hemel Hempsted/Cambridge, England) equipped with a krypton/argon laser and the necessary filter systems (fluorecein: 522DF32 and rhodamine: 585EFLP) was used to examine the stained sections. All cartilage samples were examined without knowledge of treatment and untreated regions were included within the field of view to serve as control. The maximal RFE depth (deepest point of thermal dead area), mean depth of penetration (dead area/width of dead area), percentage of RFE dead area [dead area/(dead area + live area)%], and mean cartilaginous thickness [(dead area + live area)/width of image] were determined in each confocal laser microscopy image of the osteochondral section with NIH Image software (NIH, Bethesda, MA).

HISTOLOGICAL ANALYSIS

The 2.5 mm thick cartilage slices were fixed in 10% neutral buffered formalin, then decalcified and embedded in paraffin. Five-micrometer thick sections were cut and stained with hematoxylin–eosin or Safranin-O. Cartilage thickness, chondrocyte viability, Safranin-O staining, cell morphology, cartilage structure, and tidemark integrity were assessed for each section. Cell viability was evaluated based on the information from confocal laser microscopy and added to the analysis after light microscopic data were obtained to prevent bias. Each of these characteristics was given a score according to the scoring system described in a previous study[22] (Table II). Higher scores represent better histologic appearance. Each section examined by three senior researchers without knowledge of treatment.

Data analysis

The mean and standard error of the mean (S.E.M.) were determined for cartilage thickness and chondrocyte death measurements. For subjective scores, medians and ranges were determined. Differences in maximal depth of chondrocyte death, mean depth of chondrocyte death, percentage

Table II
Light microscopic grading format

Characteristic	Score
Cartilage thickness (after treatment)	
a. >75% Normal surrounded cartilage	4
b. 50−75% Normal surrounded cartilage	3
c. 25−50% Normal surrounded cartilage	2
d. <25% Normal surrounded cartilage	1
e. Exposed calcified zone or subchondral bone	0
Cell viability in treated area evaluated by confocal microscopy (including all reparative mesenchymal cells and chondrocytes)	
a. Approximate 95−100% alive	4
b. Approximate 75−95% alive	3
c. Approximate 50−75% alive	2
d. Approximate 25−50% alive	1
e. Approximate 0−25% alive	0
Safranin-O staining	
a. Normal	4
b. Slight reduction	3
c. Moderate reduction	2
d. Severe reduction	1
e. No dye noted/no or minimal tissue	0
Cell morphology	
a. Normal	4
b. Diffuse hypercellularity	3
c. Cloning	2
d. Hypocellularity	1
e. Severe cartilage loss	0
Cartilage structure	
a. Normal	6
b. Surface irregularities	5
c. Pannus and surface irregularities	4
d. Clefts to superficial zone	3
e. Clefts to middle zone ± loss of superficial zone	2
f. Clefts to deep zone ± loss of middle zone	1
g. Absent down to the tidemark	0
Tidemark integrity	
a. Intact	2
b. Crossed by blood vessels	1
c. Severe cartilage loss (no tidemark present)	0
Perfect score	24

of dead area and mean cartilaginous thickness calculated from confocal laser microscopy image were analyzed using analysis of variance (ANOVA) (SAS, version 8.2, SAS Institute, Cary, NC). When ANOVA revealed significant differences among groups, a Duncan's multiple range test was performed to identify the differences among treatment groups. Comparison of the subjective scores among treatment groups based on gross appearance and histologic scoring systems was performed using non-parametric methods (Mann−Whitney *U* test). The material properties − aggregate modulus (H_A), Poisson's ratio (ν_s) and permeability (k) were calculated based on linear biphasic theory[34]. The effect of the experimental group and the area on the material properties and thickness of the cartilage were examined using ANOVA (SAS version 8e; SAS Institute, Cary, NC). Duncan's multiple range test was used to compare the means when the P value was significant. For all analyses, differences were considered to be significant at a probability level of 95% ($P < 0.05$). Interobserver precision error was determined among the researchers for the macroscopic surface scoring and light microscopic analysis. When comparisons were not significant, the difference (δ) between populations to detect a significant difference at power = 0.8 and $\alpha = 0.05$ was calculated.

Results

Mechanical abrasion of the patella surface followed by a 90-day postoperative exercise period resulted in a fibrillated, irregular articular surface. Macroscopically the cartilage was softened and had an irregular surface, but the soft, wispy fronds characteristic of degenerative disorders such as chondromalacia were not confluently dispersed over the entire treated surface. In some areas, cartilage loss was visible, and furrows in the cartilage caused by the abrasion tool could clearly be identified (Fig. 2). Based on macroscopic appearance at the second arthroscopy, and confocal laser microscopy of the biopsies, the model was successful in creating chondromalacia with adjacent chondrocyte death similar to previous reports[35]. However, microscopically, deep fissures were evident in the cartilage, some which penetrated as far as the subchondral bone and these fissures often resulted in large cartilage flaps being detached. Therefore, some regions were more consistent with Grade 3 chondromalacia. The surface cartilage layer was lost in the majority of samples with concomitant loss of proteoglycans confirmed through Safranin-O staining. Extensive chondrocyte cloning was localized around the fissures in the tissue (Fig. 3). These findings are more representative of a traumatic mechanical insult than the slow progressive degenerative nature often associated with malalignment or maltracking conditions of the knee and femoropatellar joint space[36]. No intraoperative or postoperative complications were encountered during the duration of the study.

Each radiofrequency device was able to contour the articular surface of the abraded patella and remove fine fibrillations. Mechanical debridement was able to contour the surface in a manner that removed the large fronds and cartilage flaps, but resulted in a surface that was mildly irregular at the completion of the debridement.

There was no difference in the cartilage thickness among treatment groups (biopsy samples before treatment) as measured by confocal laser microscopy ($P > 0.05$) (Table III). However, the treated area was thinner than the other three areas (border, superiolateral, and medial area) for all experimental groups ($P < 0.001$) with a 45−55% reduction in thickness compared to the medial area.

CoVac 50 and TAC-CII treatments resulted in twice the maximum depth of chondrocyte death compared with

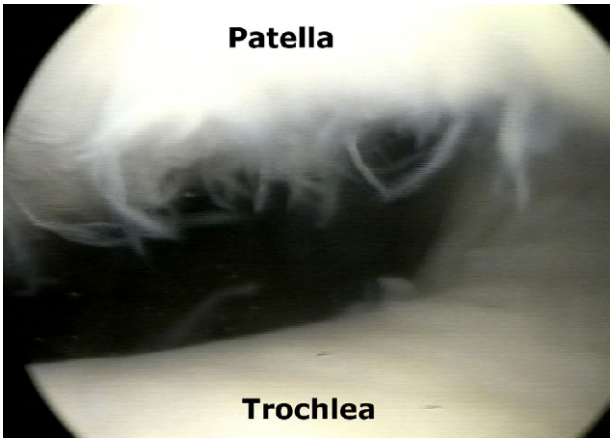

Fig. 2. Arthroscopic image of the articular surface of the patella (top of photo) demonstrating the partial thickness cartilage injury prior to treatment.

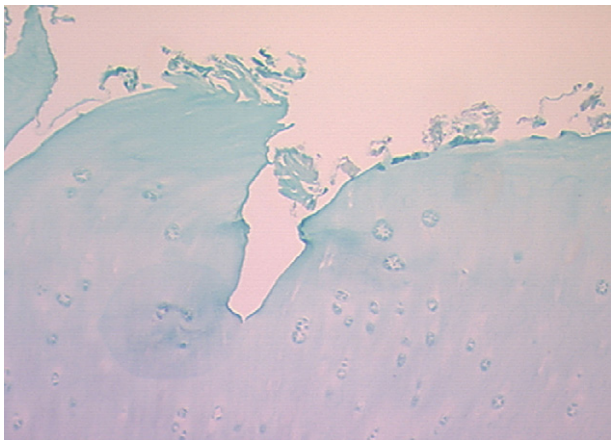

Fig. 3. Safranin-O stained light microscopy of osteochondral section from control animal. This image demonstrates surface fibrillation, chondrocyte cloning, and loss of proteoglycan staining. Articular surface is toward the top (original 200×).

mechanical debridement ($P < 0.05$) (Table III), and 3.5–4.6 times the mean depth and area of chondrocyte death compared with mechanical debridement ($P < 0.05$) (Table III) [Fig. 4(A–D)]. In addition, reduced viability, loss of Safranin-O staining, and abnormal cell morphology resulted in lower individual and total light microscopy scores for the RFE treated groups compared to control and mechanically debrided areas ($P < 0.05$) (Table IV) [Fig. 5(A–D)]. There was no difference in cartilage structure (surface topography) among the experimental groups ($P > 0.05$) (Table IV). There was no difference in the cartilage surface scores among the treatment groups; MD = 1.3 (0, 3.1) (median, range); CoVac 50 = 1.2 (0.0, 3.1); TAC-CII = 1.0 (0.1, 2.7) and control = 2.5, (1.3, 3.3) samples ($P > 0.05$). The intraobserver and interobserver precision errors for macroscopic surface scores were 23.4% (Grade = 0.4) and 24.1% (Grade = 0.4), respectively.

There were no significant differences in the aggregate modulus among experimental groups in treated, border or medial areas. However, the superior–lateral area of the TAC-CII group showed a significantly lower aggregate modulus compared to the other groups. Within each experimental group, aggregate modulus values significantly differed among the four areas ($P < 0.0001$). The medial area had the highest aggregate modulus in all groups while the treated area showed the lowest value. Treated and border areas showed an approximately 60–75% decrease in aggregate modulus compared to that of medial area. There were no significant differences in aggregate modulus between the treated and border areas in any of the experimental groups (Table V). The aggregate modulus values of superior–lateral areas were 30–40% less than that of medial area. The Poisson's ratio was significantly higher in the treated area compared to other areas in all experimental groups. In all of the experimental groups except the control group, the permeability values were higher in the treated area compared to other three areas. Within the experimental groups, except for the control group, the superior–lateral area showed significantly lower permeability value compared to the treated area. Except the border area, none of the tested areas showed any significant influence of the type of treatment in permeability values.

Table III
Cartilage thickness, maximum and mean depth of chondrocyte death, and area of chondrocyte death

	Cartilage thickness (μm) before treatment	Chondrocyte death after treatment		
		Mean (μm)	Maximum (μm)	Area (%)
Control	1308 ± 116^a	207 ± 54^a	764 ± 110^a	17 ± 5^a
Mechanical debridement	1367 ± 152^a	166 ± 34^a	586 ± 63^a	13 ± 3^a
CoVac 50	1122 ± 81^a	609 ± 122^b	1162 ± 364^b	55 ± 10^b
TAC-CII	1320 ± 141^a	735 ± 58^b	1187 ± 83^b	60 ± 7^b

Values represent means ± S.E.M. Different superscript letters within a column represent differences among groups ($P < 0.05$).

Discussion

This study aimed to develop an animal model of cartilage injury (partial thickness cartilage fibrillation) that would be representative of the clinical situation and could be used to compare the treatments of mechanical debridement and RFE with particular attention paid to contouring the damaged articular surface, the effects on chondrocyte viability, and the long-term histologic and mechanical characteristics of the cartilage matrix. A pony model was selected due to the joint similarities with that of the human in terms of overall size, thickness of the articular cartilage, forces acting on joint surfaces and degenerative disease progression[37]. The joint size also allows the use of clinically applicable probes and arthroscopy systems as well as *in vivo* indentation testing devices. However, the RFE settings recommended by manufacturers used in this study were for human patients, they may not be optimal for the treatment of horses because of the different body size and weight between humans and horses. Differences were found between the experimentally created model of cartilage injury used in this study and some injuries seen clinically, thus emphasizing the limitations and difficulties in developing animal models which are representative of the clinical situation. Specifically, the model developed in this study was more representative of a traumatic insult than the slow, progressive degeneration associated with clinical changes seen in maltracking or malalignment leading to chondromalacia patella. Macroscopically, deep furrows were visible which correlated with the coarseness of the abrasion tool and histologically chondral fractures were observed which in some cases extended down to the subchondral bone (ICRS Grade 3b)[38].

In this study, the cartilage surface was macroscopically smoothed with each RFE device during arthroscopy in a manner that was visually superior at surgery compared with mechanical shaving, however, this visual effect was not maintained over the 22 month duration of this study. In addition, there were no morphometric or biomechanical differences among the four experimental groups and overall morphometric scores for all groups were low indicating the aggressive nature of the model. Furthermore, extensive cell death associated with the RFE treatments occurred in this study. Lu *et al.* [21,22,24,32,39–41] have demonstrated chondrocyte death, including the penetration of the subchondral bone with application of both monopolar and bipolar RFE. Others have questioned the validity of these studies[18], specifically the significance of viability testing at time zero compared to viability over time after thermal exposure. Recently, Kaab *et al.*[16] also demonstrated that RFE

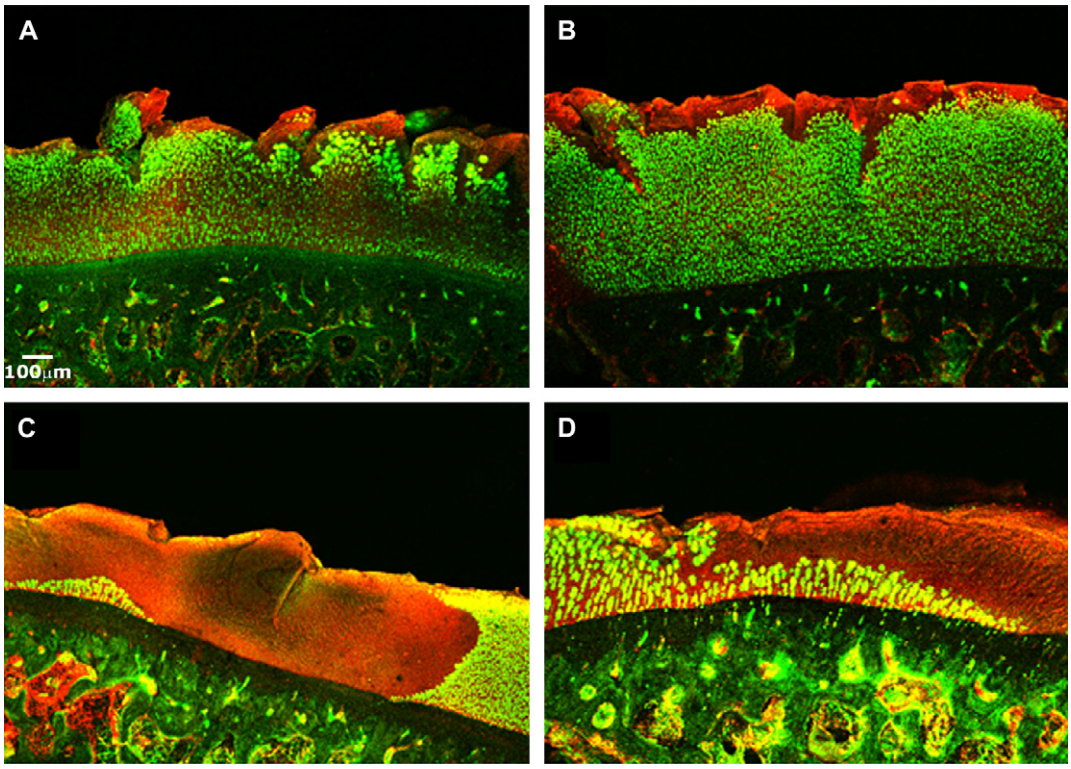

Fig. 4. Collage of the confocal laser microscopy images demonstrating increased cell death for both bRFE and mRFE compared to control and mechanical debridement. Confocal laser microscopy and vital cell staining of osteochondral sections, articular surface is toward the top (original 20×). Green dots are viable cells, red dots are dead cells. A: Control; B: mechanical debridement; C: CoVac 50 probe coupled with ArthroCare 2000 generator; D: TAC-CII probe coupled with Vulcan EAS generator.

caused thermal damage to cartilage 24 weeks after application in a sheep model as previously reported by Lu *et al.*[22]. In addition, Caffey *et al.* evaluated five RFE systems currently on the market to determine the thermal effects on human articular cartilage[42]. The results of his study showed significant cellular death caused by these RFE systems.

The regions with partial thickness cartilage loss and fibrillation had inferior mechanical properties in the area of abrasion compared to the non-abraded area. The indentation response of articular cartilage is dependent upon the high tensile stiffness of the superficial collagen layer, in addition to the compressive stiffness provided by proteoglycans in the matrix[43]. The superficial collagen layer was damaged in all the groups in the study, which is partially responsible for the reduced stiffness properties demonstrated in the treated area. In healthy cartilage during loading, the surface zone and the intermediate zone form a common functional unit providing a high degree of fiber cross linkage to increase zonal compressive stiffness, and an intact superficial zone helps prevent peaks of surface tensile strain[44]. The greatly diminished flow-dependent mechanisms of load support due to loss of upper layers of cartilage can lead to increased stress on the solid matrix, a decrease in elastic modulus of collagen and fibril lengths and resultant cyclic fatigue[45,46]. The results reported here also suggest a gradient change in mechanical properties while moving away from the treated area, with the highest stiffness in the area farthest from the damaged portion. Progression of cartilage degeneration from focal areas of damage to the adjoining areas due to the release of inflammatory agents is well established[45,46]. The stiffness in articular cartilage after RFE treatment to be decreased compared to normal healthy cartilage has been reported by Uthamanthil *et al.*[31].

The thickness of the injured area was lower compared to other areas of untreated cartilage in all groups, although it is a limitation of this study that no baseline thickness measurements were taken prior to injuring the tissue. Thinning of injured cartilage is known to occur after injury[47]. Thinning in all groups may be due to continual degeneration of the

Table IV
Light microscopic analysis of thickness, visibility, Safranin-O staining, morphology, structure, and tide-mark integrity

	Thickness	Viability	Safranin-O	Morphology	Structure	Tide-mark integrity	Total
Control	3.0 (1.0, 3.7)[a]	3.0 (2.3, 3.3)[a]	2.5 (1.7, 3.0)[a]	2.0 (1.8, 2.0)[a]	1.7 (1.0, 2.0)[a]	1.9 (1.0, 2.0)[a]	13.3 (10.2, 15.3)[a]
Mechanical debridement	3.0 (1.7, 3.7)[a]	3.0 (2.3, 3.0)[a]	2.2 (1.3, 3.0)[a]	2.0 (1.8, 2.0)[a]	1.7 (1.0, 2.3)[a]	2.0 (1.0, 2.0)[a]	13.8 (9.8, 16.0)[a]
CoVac 50	2.8 (1.7, 3.3)[a]	0.5 (0.0, 2.3)[b]	1.2 (0.0, 2.3)[b]	1.1 (0.7, 1.7)[b]	1.7 (1.0, 3.3)[a]	2.0 (1.0, 2.0)[a]	8.4 (5.3, 13.3)[b]
TAC-CII	3.0 (1.7, 3.3)[a]	1.5 (0.0, 2.3)[b]	1.3 (0.3, 2.0)[b]	1.5 (0.7, 1.8)[b]	1.2 (0.7, 2.0)[a]	1.5 (1.0, 2.0)[a]	9.2 (5.2, 12.8)[b]

Values represent median, range. Different superscript letters within a column represent differences among groups ($P < 0.05$).

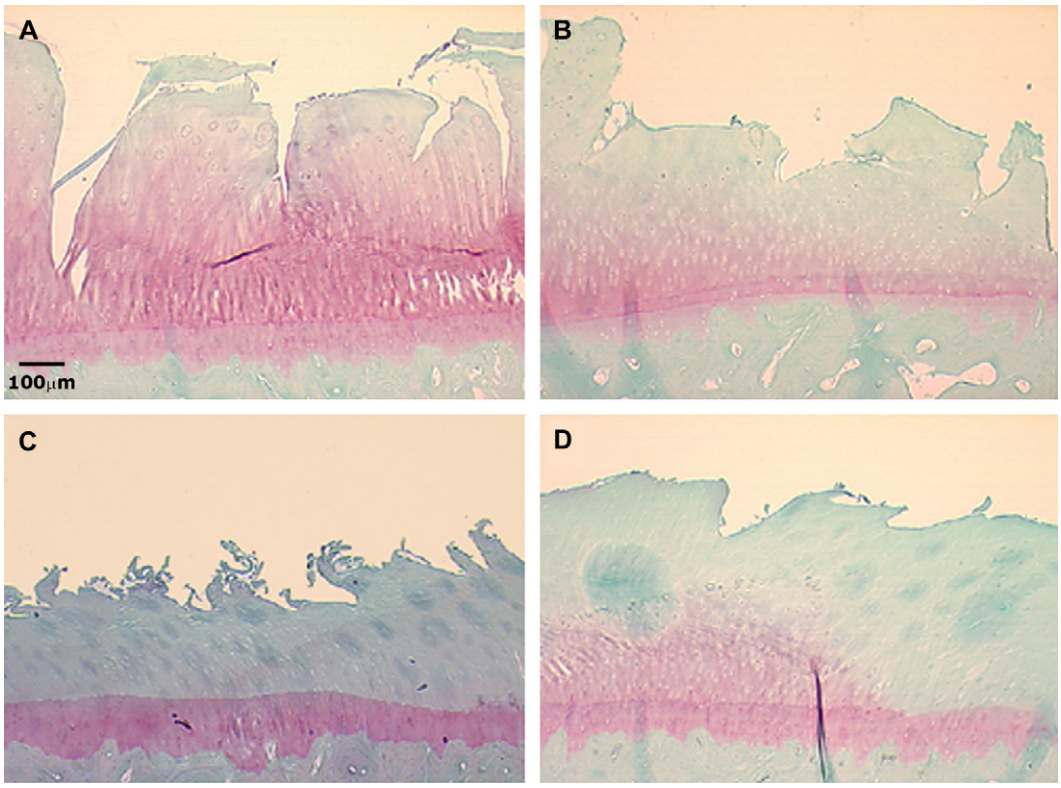

Fig. 5. Collage of histologic images of osteochondral sections from each group at the endpoint of the experiment. Articular surface is toward the top (Safranin-O staining, original 40×). A: Control; B: mechanical debridement; C: CoVac 50 probe coupled with ArthroCare 2000 generator; D: TAC-CII probe coupled with Vulcan EAS generator.

cartilage associated with loss of proteoglycans and collagen denaturation further exacerbated by chondrocyte apoptosis and necrosis[7]. It is surprising that the loss of thickness was not greater in the mechanical debridement group due to actual removal of tissue during the treatment process. In the RFE treated groups, collagen shrinkage due to heating and RFE ablation may also have played a role in cartilage thinning. Hogan and Diduch also reported a case of progressive thinning of cartilage after treatment with RFE[48].

Table V
Biomechanical characteristics of the treated and untreated patellar regions

Experimental Group	Treated (T)	Border (B)	Superiolateral (S)	Medial (M)
Aggregate modulus H_A (MPa)				
Control	$0.155 \pm 0.035^{a,*}$	$0.213 \pm 0.069^{a,*}$	$0.303 \pm 0.103^{b,*,**}$	$0.428 \pm 0.114^{c,*}$
MD	$0.190 \pm 0.100^{a,*}$	$0.206 \pm 0.047^{a,*}$	$0.274 \pm 0.019^{b,*,**}$	$0.448 \pm 0.048^{c,*}$
TAC-CII	$0.163 \pm 0.060^{a,*}$	$0.185 \pm 0.074^{a,*}$	$0.244 \pm 0.042^{b,*}$	$0.411 \pm 0.146^{c,*}$
CoVac 50	$0.148 \pm 0.045^{a,*}$	$0.185 \pm 0.092^{a,*}$	$0.323 \pm 0.067^{b,**}$	$0.521 \pm 0.076^{c,*}$
Permeability k ($m^4/N\,s \times 10^{-15}$)				
Control	$2.906 \pm 1.004^{a,*}$	$2.922 \pm 0.550^{a,*,**}$	$2.658 \pm 0.548^{a,*}$	$3.238 \pm 0.764^{a,*}$
MD	$3.544 \pm 1.368^{a,*}$	$2.435 \pm 0.653^{b,*}$	$2.407 \pm 0.470^{b,*}$	$2.812 \pm 0.656^{a,b,*}$
TAC-CII	$5.520 \pm 4.363^{a,*}$	$3.357 \pm 0.979^{a,b,*,**}$	$2.569 \pm 1.021^{b,*}$	$3.507 \pm 1.097^{a,b,*}$
CoVac 50	$4.718 \pm 2.994^{a,*}$	$4.253 \pm 2.981^{a,b,**}$	$2.126 \pm 0.715^{b,*}$	$2.731 \pm 0.562^{a,b,*}$
Poisson's ratio ν_s				
Control	$0.039 \pm 0.052^{a,*}$	$0.00^{b,*}$	$0.00^{b,*}$	$0.00^{b,*}$
MD	$0.045 \pm 0.063^{a,*}$	$0.00^{b,*}$	$0.00^{b,*}$	$0.00^{b,*}$
TAC-CII	$0.030 \pm 0.050^{a,*}$	$0.00^{b,*}$	$0.001 \pm 0.003^{b,*}$	$0.00^{b,*}$
CoVac 50	$0.035 \pm 0.038^{a,*}$	$0.008 \pm 0.024^{b,*}$	$0.00^{b,*}$	$0.00^{b,*}$
Thickness h (mm)				
Control	$0.96 \pm 0.39^{a*}$	$1.49 \pm 0.35^{b,*}$	$1.64 \pm 0.41^{b,*}$	$1.74 \pm 0.28^{b,*}$
MD	$0.99 \pm 0.65^{a*}$	$1.51 \pm 0.35^{b,*}$	$1.86 \pm 0.38^{b,*}$	$1.88 \pm 0.38^{b,*}$
TAC-CII	$0.85 \pm 0.38^{a*}$	$1.19 \pm 0.39^{a*}$	$1.85 \pm 0.42^{b,*}$	$1.72 \pm 0.34^{b,*}$
CoVac 50	$0.75 \pm 0.32^{a*}$	$1.46 \pm 0.37^{b,*}$	$1.73 \pm 0.37^{b,*}$	$1.68 \pm 0.29^{b,*}$

Values represent mean ± S.E.M. Values within a row with superscripts of differing letters are significantly different. Values within a column with differing number of asterisks (*, **) are significantly different. Significance $P < 0.05$.

A surprising result was that there were no significant differences among the groups in the permeability of treated and untreated areas as a previous study reported[31]. The reason for this may be due to the sensitivity of the biomechanical test used in this study, which may not be sufficient to show differences between the groups. Other biomechanical tests may be capable of distinguishing the differences among the groups. There has been much discussion about the ability of RFE to anneal and seal the cartilage surface; however, it is yet to be determined whether the ability to seal the cartilage surface has any benefit, as it would be a balance between preventing the release of degenerative cytokines from the injured cartilage and detrimental effects on nutrient flow and pH. In a recent study, a decrease in permeability of the matrix was observed immediately after treatment with RFE on osteoarthritic femoral articular cartilage[49].

Lu *et al.* demonstrated in a sheep model of a focal defect in a non-load-bearing site that RFE was able to stabilize the articular cartilage and maintain a non-fissured surface 6 months after treatment in spite of full thickness chondrocyte death[22]. However, in this model at 22 months, the cartilage surface of RFE treated regions was as fibrillated as the untreated controls and mechanically debrided regions. It is possible that several factors caused the recurrence or persistence of the microscopic fibrillation identified on light microscopy in this study. First, the tool used to abrade the cartilage surface created wide clefts with cartilage loss in some instances and chondral fracture that extended deep into the cartilage matrix. Light intermittent application of RFE may not have sealed or annealed the articular surface and remaining clefts may have propagated over time, furthermore over treatment may have occurred in an attempt to smooth the surface, resulting in further deleterious effects on cell viability. Even more aggressive treatment with the RFE devices may have prevented continued fibrillation from occurring, but would have most likely resulted in more extensive chondrocyte death[24]. In addition, the denaturation of collagen in the matrix may have led to weakening of the articular cartilage and subsequent matrix fissuring.

Similar to previously published *in vitro* work, RFE treatment resulted in loss of matrix staining for proteoglycans using Safranin-O[22,24]. This is most likely caused by a combination of factors. Abrasion of the cartilage surface and disruption of the normal collagen architecture results in altered matrix biomechanical characteristics and in loss of proteoglycans. In addition, based on the *in vitro* studies and loss of proteoglycans staining with RFE treatment alone[22,24], it is likely that thermal denaturation of proteoglycans occurs during treatment and massive chondrocyte loss prevents proteoglycan replacement within the treated matrix. The loss of proteoglycan correlates with the inability of RFE to seal the cartilage surface in this model and the lack of increased chondrocyte metabolism at the margins of injury as reported by Hunziker and Quinn[50].

Caution should be used when using RFE probes for treating articular cartilage with large clefts that penetrate deep into the tissue. However, RFE may have a role to play in treatment of injured articular cartilage, particularly in the light of the symptomatic relief given to patients, the ability to smooth the surface initially without removal of uninjured tissue and the ability to maintain function even in the presence of full thickness cell death in a non-load-bearing site. Ongoing research and reports document that the depth of chondrocyte injury can be controlled in part by modifying RFE probe design[25]. Moreover, future studies are required to further develop animal models that are more representative of the clinical situation.

One important limitation of this study merits discussion. There was not a control group that was euthanized at the time of the second surgery to assess the cartilage biomechanics and detailed light microscopy of the injured cartilage prior to treatment to give baseline measurements on the degeneration of the tissue. Therefore, it cannot be confirmed that this damage was a direct result of the mechanical abrasion and not a result of the applied treatment, however the untreated controls were found to have similar macroscopic and histological characteristics to all the three treatment groups.

The ability to induce cartilage defects representative of clinical situation remains an experimental challenge. In this study, the aggressive cartilage injury resulted in defects with deeper crevices and larger fibrillations than what is typically seen clinically in Grade 2 chondromalacia and chondromalacia associated with malalignment and maltracking, however, it is consistent with Grade 3 cartilage injury, a partial thickness lesion that warrants investigation. The clinical use of current RFE devices for the management of severely damaged articular cartilage should be approached with caution. However, the enticing visual effects, the ability to smooth the articular cartilage surface in manner far superior to that of motorized shaving and the lack of any other viable alternative indicates that further work is warranted to determine what parameters exist and if the probes or power generators can be modified to optimize clinical application of thermal chondroplasty.

References

1. Curl WW, Krome J, Gordon ES, Rushing J, Smith BP, Poehling GG. Cartilage injuries: a review of 31,516 knee arthroscopies. Arthroscopy 1997;13:456–60.
2. O'Driscoll SW. The healing and regeneration of articular cartilage. J Bone Joint Surg Am 1998;80:1795–812.
3. Buckwalter JA, Mankin HJ. Articular cartilage. Part I: tissue design and chondrocyte–matrix interactions. J Bone Joint Surg Am 1997;79:600–11.
4. Buckwalter JA, Lane NE. Athletics and osteoarthritis. Am J Sports Med 1997;25:873–81.
5. Buckwalter JA, Mankin HJ. Articular cartilage repair and transplantation. Arthritis Rheum 1998;41:1331–42.
6. Sgaglione NA, Miniaci A, Gillogly SD, Carter TR. Update on advanced surgical techniques in the treatment of traumatic focal articular cartilage lesions in the knee. Arthroscopy 2002;18:9–32.
7. Hunziker EB. Articular cartilage repair: basic science and clinical progress. A review of the current status and prospects. Osteoarthritis Cartilage 2002;10:432–63.
8. Hunziker EB. Biologic repair of articular cartilage. Defect models in experimental animals and matrix requirements. Clin Orthop 1999;367(Suppl):S135–46.
9. Pritzker KP. Animal models for osteoarthritis: processes, problems and prospects. Ann Rheum Dis 1994;53:406–20.
10. Breinan HA, Hsu HP, Spector M. Chondral defects in animal models: effects of selected repair procedures in canines. Clin Orthop 2001;391(Suppl):S219–30.
11. Barber FA, Uribe JW, Weber SC. Current applications for arthroscopic thermal surgery. Arthroscopy 2002;18:40–50.
12. Oloff LM, Bocko AP, Fanton G. Arthroscopic monopolar radiofrequency thermal stabilization for chronic lateral ankle instability: a preliminary report on 10 cases. J Foot Ankle Surg 2000;39:144–53.

13. Tasto JP, Ash SA. Current uses of radiofrequency energy in arthroscopic knee surgery. Am J Knee Surg 1999;12:186–91.
14. Uribe JW. Electrothermal chondroplasty – bipolar. Clin Sports Med 2002;21:675–85.
15. Khan AM, Dillingham MF. Electrothermal chondroplasty – monopolar. Clin Sports Med 2002;21:663–74.
16. Kaab MJ, Bail HJ, Rotter A, Mainil-Varlet P, apGwynn I, Weiler A. Monopolar radiofrequency treatment of partial-thickness cartilage defects in the sheep knee joint leads to extended cartilage injury. Am J Sports Med 2005;33:1472–8.
17. Owens BD, Stickles BJ, Balikian P, Busconi BD. Prospective analysis of radiofrequency versus mechanical debridement of isolated patellar chondral lesions. Arthroscopy 2002;18:151–5.
18. Yetkinler DN, Greenleaf JE, Sherman OH. Histologic analysis of radiofrequency energy chondroplasty. Clin Sports Med 2002;21:649–61.
19. Yetkinler DN, McCarthy EF. The use of live/dead cell viability stains with confocal microscopy in cartilage research. Sci Bull 2000;1:1–2.
20. Turner AS, Tippett JW, Powers BE, Dewell RD, Hallinckrodt CH. Radiofrequency (electrosurgical) ablation of articular cartilage. A study in sheep. Arthroscopy 1998;14:585–91.
21. Lu Y, Edwards RB, Cole BJ, Markel MD. Thermal chondroplasty with radiofrequency energy: an *in vitro* comparison of bipolar and monopolar radiofrequency devices. Am J Sports Med 2001;29:42–9.
22. Lu Y, Hayashi K, Hecht P, Fanton GS, Thabit G, Cooley AJ, *et al*. The effect of monopolar radiofrequency energy on partial-thickness defects of articular cartilage. Arthroscopy 2000;16:527–36.
23. Edwards RB, Lu Y, Rodriguez E, Markel MD. Thermometric determination of cartilage matrix temperatures during thermal chondroplasty: comparison of bipolar and monopolar radiofrequency devices. Arthroscopy 2002;18:339–46.
24. Edwards RB, Lu Y, Kalscheur VL, Nho S, Cole BJ, Markel MD. Thermal chondroplasty of chondromalacic human cartilage: an *ex vivo* comparison of bipolar and monopolar radiofrequency devices. Am J Sports Med 2002;30:90–7.
25. Meyer ML, Lu Y, Markel MD. Effects of radiofrequency energy on human chondromalacic cartilage: an assessment of insulation material properties. IEEE Trans Biomed Eng 2005;52:702–10.
26. Cook JL, Kuroki K, Kenter K, Marberry K, Brawner T, Geiger T, *et al*. Bipolar and monopolar radiofrequency treatment of osteoarthritic knee articular cartilage: acute and temporal effects on cartilage compressive stiffness, permeability, cell synthesis, and extracellular matrix composition. J Knee Surg 2004;17:99–108.
27. Moustafa MAI, Boero MJ, Baker GJ. Arthroscopic evaluation of the femorotibial joints of horses. Vet Surg 1987;16:352–7.
28. Peroni JF, Stick JA. Evaluation of a cranial arthroscopic approach to the stifle joint for the treatment of femorotibial joint disease in horses: 23 cases (1998–1999). J Am Vet Med Assoc 2002;220:1046–52.
29. Athanasiou KA, Agarwal A, Muffoletto A, Dzida FJ, Constantinides MS, Clem M. Biomechanical properties of hip cartilage in experimental animal models. Clin Orthop 1995;316:254–66.
30. Athanasiou KA, Agarwal A, Dzida FJ. A comparative study of the intrinsic mechanical properties of the human acetabular and femoral head cartilage. J Orthop Res 1994;12:340–9.
31. Uthamanthil RK, Edwards RB, Lu Y, Manley PA, Athanasiou KA, Markel MD. An *in vivo* study on the short term effect of radiofrequency energy on chondromalacic patellar cartilage and its correlation with calcified cartilage pathology in an equine model. J Orthop Res 2006;24:716–24.
32. Lu Y, Edwards RB, Kalscheur VL, Nho S, Cole BJ, Markel MD. Effect of bipolar radiofrequency energy on human articular cartilage: comparison of confocal laser microscopy and light microscopy. Arthroscopy 2001;17:117–23.
33. Mainil-Varlet P, Monin D, Weiler C, Grogan S, Schaffner T, Zuger B, *et al*. Quantification of laser-induced cartilage injury by confocal microscopy in an *ex vivo* model. J Bone Joint Surg Am 2001;83:566–71.
34. Mow VC, Kuei SC, Lai WM, Armstrong CG. Biphasic creep and stress relaxation of articular cartilage in compression: theory and experiments. J Biomech Eng 1980;102:73–84.
35. Tew SR, Kwan AP, Hann A, Thomson BM, Archer CW. The reactions of articular cartilage to experimental wounding: role of apoptosis. Arthritis Rheum 2000;43:215–25.
36. Mori Y, Kubo M, Okumo H, Kuroki Y. Histological comparison of patellar cartilage degeneration between chondromalacia in youth and osteoarthritis in aging. Knee Surg Sports Traumatol Arthrosc 1995;3:167–72.
37. Athanasiou KA, Rosenwasser MP, Buckwalter JA, Malinin TI, Mow VC. Interspecies comparisons of *in situ* intrinsic mechanical properties of distal femoral cartilage. J Orthop Res 1991;9:330–40.
38. Brittberg M, Winalski CS. Evaluation of cartilage injuries and repair. J Bone Joint Surg Am 2003;85(Suppl 2): 58–69.
39. Edwards RB III, Lu Y, Markel MD. The basic science of thermally assisted chondroplasty. Clin Sports Med 2002;21:619–47.
40. Lu Y, Hayashi K, Edwards III, Fanton GS, Thabit III, Markel MD. The effect of monopolar radiofrequency treatment pattern on joint capsular healing: *in vitro* and *in vivo* studies using an ovine model. Am J Sports Med 2000;28:711–9.
41. Lu Y, Edwards RB, Nho S, Cole BJ, Markel MD. Lavage solution temperature influences depth of chondrocyte death and surface contouring during thermal chondroplasty with temperature controlled monopolar radiofrequency energy. Am J Sports Med 2002;30:667–73.
42. Caffey S, McPherson E, Moore B, Hedman T, Vangsness CT Jr. Effects of radiofrequency energy on human articular cartilage: an analysis of 5 systems. Am J Sports Med 2005;33:1035–9.
43. Kovach IS, Athanasiou KA. Small-angle HeNe laser light scatter and the compressive modulus of articular cartilage. J Orthop Res 1997;15:437–41.
44. Glaser C, Putz R. Functional anatomy of articular cartilage under compressive loading. Quantitative aspects of global, local and zonal reactions of the collagenous network with respect to the surface integrity. Osteoarthritis Cartilage 2002;10:83–99.
45. Smith MD, Triantafillou S, Parker A, Youssef PP, Coleman M. Synovial membrane inflammation and cytokine production in patients with early osteoarthritis. J Rheumatol 1997;24:365–71.
46. Hedbom E, Hauselmann HJ. Molecular aspects of pathogenesis in osteoarthritis: the role of inflammation. Cell Mol Life Sci 2002;59:45–53.

47. Ewers BJ, Weaver BT, Sevensma ET, Haut RC. Chronic changes in rabbit retro-patellar cartilage and subchondral bone after blunt impact loading of the patellofemoral joint. J Orthop Res 2002;20: 545–50.
48. Hogan CJ, Diduch DR. Progressive articular cartilage loss following radiofrequency treatment of a partial-thickness lesion. Arthroscopy 2001;17:E24.
49. Cook JL, Marberry KM, Kuroki K, Kenter K. Assessment of cellular, biochemical, and histologic effects of bipolar radiofrequency treatment of canine articular cartilage. Am J Vet Res 2004;65:604–9.
50. Hunziker EB, Quinn TM. Surgical removal of articular cartilage leads to loss of chondrocytes from cartilage bordering the wound edge. J Bone Joint Surg Am 2003;85(Suppl 2):85–92.